
Article:
Leong, Z., Holmes, W., Clarke, J. et al. (2019) Magnetostrictive sensors for composite damage detection and wireless structural health monitoring. IEEE Transactions on Magnetics, 55 (7). 4003006. ISSN: 0018-9464

https://doi.org/10.1109/TMAG.2019.2899537

Magnetostrictive sensors for composite damage detection and wireless structural health monitoring

Zhaoyuan Leong, William Holmes, James Clarke, Akshay Padki, Simon Hayes, and Nicola A Morley, *Member, IEEE*

Department of Materials Science and Engineering, University of Sheffield, Sheffield, UK S1 3JD

The efficacy of magnetostrictive ribbon actuators as aerospace composites impact damage detectors have been investigated through finite element modelling and experimental studies, investigating both the sensitivity of magnetostrictive ribbons embedded and surface mounted using tensile and 3-point bending tests. From the modelling, it was found that the surface mounted ribbons increased the Young's modulus of the system compared to the composite alone, but caused the ribbons to delaminate from the surface before failure. The embedded ribbons did not appear to affect the structural properties of the composite, which was observed through the 3-point bending tests carried out. From the impact damage tests, it was determined that the ribbons had to be embedded 2-ply below the surface to measure impact energies greater than 1.6J. For surface mounted ribbons, damages of 1.6J to the surface could be detected and pinpointed for two ribbons 10mm apart. We also demonstrate in a simple way how a two-ribbon scheme may be used to determine damage position in the tested sample, which may be extended for wireless sensing.

***Index Terms*— Impact damage, magnetostriction, Composite damage detection, Non-destructive testing**

I. Introduction

As the aerospace industry strives for cheaper, lighter, and more efficient aircraft, the use of carbon fibre reinforced polymer (CFRP) composite within the main structure has become more common [1], with modern aircraft consisting of up to 50% composite materials [2]. One of the disadvantages of composites are owing to their complex laminate structures, their failure mechanisms [3] are more complicated than classic aircraft materials such as metals: detecting and monitoring the different forms of composite damage is thus important to ensure that failure of components does not occur during its operational lifetime [3].

Damage often occurs during service, for example due to low velocity impacts caused by service personnel dropping tools or birds - this type of impact results in barely visible damage (BVD). There are a range of different damage mechanisms that occur in composites due to BVD [3, 4], these include delamination of the composite ply, micro-cracking in both the matrix and fibres and deboning between fibres and matrix. BVD may be difficult to detect visually, therefore high-sensitivity non-destructive testing (NDT) methods are required to monitor the composite for damage [5]; examples of such techniques are ultrasonic testing, infra-red testing, and radiographic testing [6, 7]. Recently the feasibility of *in-situ* structural health monitoring (SHM) has been investigated [8]. This involves arrays of sensors permanently attached to the composite components, which can constantly monitor the composite. This in turn reduces the down-time of the aircraft, eliminates component tear down, thus avoiding operational failure. The most popular SHM methods are optical-fibre Bragg gratings [9-12], which can either be surface mounted or embedded in the composite, and surface mounted piezoelectric sensors [13, 14].

Another option is magnetostrictive actuators, with built-in wireless sensors [15]. Magnetostrictive materials change their magnetisation under applied stress, which makes them ideal for detecting BVD in composites, as the damage produced induces a strain field within the composite. Early work [15, 16] demonstrated that embedded magnetostrictive wires in composite could detect uniform strain [15] and that the sensitivity is comparable with other SHM systems [16]. More recent work has shown that magnetostrictive ribbons have a better sensitivity to uniform strain compared to magnetostrictive wires [17]. This is due to the larger surface area of the ribbon. The distance between the ribbons in the actuator lay-up affects strain sensitivity, with greater sensitivity as the ribbons are located closer. A trade-off between actuator sensitivity and composite weight must therefore be reached. This paper presents further research on the ideal ribbon actuator lay-up for impact damage. ABAQUS software (commonly used in the aerospace industrial sector) was used to model ribbons either mounted on the surface or embedded in the composite, to help understand what happens in the system under uniform strain. Complementary experimental work was also performed to study the response of the magnetostrictive ribbons to impact damage and 3-point bending measurements for ribbons attached to the surface and embedded in the composite.

Manuscript received April 1, 2015; revised May 15, 2015 and June 1, 2015; accepted July 1, 2015. Date of publication July 10, 2015; date of current version July 31, 2015. (Dates will be inserted by IEEE; "published" is the date the accepted preprint is posted on IEEE Xplore®; "current version" is the date the typeset version is posted on Xplore®). Corresponding author: F. A. Author (e-mail: f.author@nist.gov). If some authors contributed equally, write here, "F. A. Author and S. B. Author contributed equally." IEEE Transactions on Magnetics discourages courtesy authorship; please use the Acknowledgment section to thank your colleagues for routine contributions.

Color versions of one or more of the figures in this paper are available online at http://ieeexplore.ieee.org.

Digital Object Identifier (inserted by IEEE).

II. Experimental Procedures

A. ABAQUS Modelling

Within the aerospace industry, the finite element analysis (FEA) software ABAQUS is used to model composite components to understand how they behaviour under different forms of strain/stress, including uniform strain and impact damage. To gain a deeper understanding of how the magnetostrictive wires and ribbons, which have previously been measured [17] on the composite surface and within the composite for both uniform tensile stress and 3-point bending measurements, these systems were modelled within the ABAQUS software. Fig. 1 shows the ABAQUS models for the tensile test with the ribbons on the surface and the 3-point bending with the ribbons within the composite. For each model, the composite consisted of 4-ply composites with 3mm wide magnetostrictive ribbons running parallel to each other with a 10mm gap between them. Each composite ply was taken to be 0.3mm thick – this is in good agreement with the measured experimental thickness of the 4-ply samples @ 1.4 mm, with Young's modulus of 52.9 GPa in-plane, while the ribbon was taken to be 200 µm thick, with Young's modulus of 168 GPa. The direction of the ply is shown in Fig. 1a. The models were run for no ribbons, with ribbons attached to the surface, and ribbons embedded between the second and third layer of the composite. An axis of symmetry was set-up in the model to allow for a finer mesh and faster computational time. For the tensile test and the 3-point bending measurements, the size of the composite modelled was 15×5 cm.

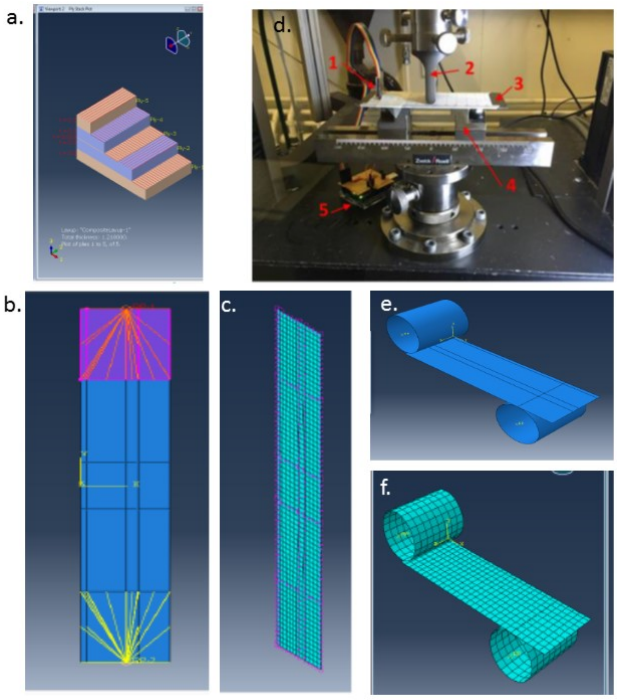

Fig. 1. ABAQUS modelling set-up a. the lay-up of the composite ply, b. the symmetry axis, along with the boundary conditions for the tensile test, c. the mesh for the ribbons mounted on the surface for the tensile test, d. the 3-point bending test for the composite, e. the symmetry axes for the 3-point bending and f. the mesh for the 3-point bending.

B. Experimental Set-Up

For the experimental measurements, the composite used was the VTC401® twill weave prepreg from SHD Composite Materials Ltd. The magnetotstrictive ribbons used are amorphous CoSiB ribbons from Vacuumschmelze with width 3 mm and 200 µm in thickness. All the samples were laid up by hand, with Table 1 summarising the different samples studied. The ribbons were arranged between the centre two plys of the prepreg, or onto the prepreg surface and were co-cured in a vacuum autoclave for 45 mins @ 100 °C.

TABLE I
SUMMARY OF THE MAGNETOSTRICTIVE RIBBON-COMPOSITE SAMPLES STUDIED

Composite lay-up	Magnetostrictive ribbon position	Dimensions (mm)	Experiments
4-ply	Embedded between plys 2-3	150×50	Impact, 3-point bending
6-ply	Embedded between plys 3-4	150×50	Impact, 3-point bending
8-ply	Embedded between plys 5-6	150×50	Impact, 3-point bending
4-ply	Single surface mounted ribbon	100×50	Impact
4-ply	Two surface mounted ribbons, 10mm apart	150×50	Impact

To determine the efficacy of the fabricated actuators for BVD detection, a series of different impact measurements were carried out *via* drop tests to induce impact damage, where the impact energy is varied by either changing the height and/or weight of the 3mm ø impact tip (detailed below). Two different impact studies were carried out: the first investigated the sensitivity of the magnetostrictive ribbon embedded at the centre of different thickness plys with impact energies ranging from 0.84-4.10 J. The second study investigated the magnetisation response of either one or two magnetostrictive ribbons mounted on the composite surface as a function of impact energy and distance of impact from the ribbons. These sets of studies were designed to determine the optimum design for the magnetostrictive actuators utilising a HMC5883L AMR sensor to determine magnetisation values. For single ribbon measurements, the magnetisation of the ribbon was taken at the closest point to the damage and along the ribbon, while for the two surface-mounted ribbon measurements, the ribbons were 10mm apart, and magnetisation measurements were taken directly above the centre of either ribbon.

Three-point bending measurements were carried out using a Zwick-Roell static materials testing machine. These measurements were done to compare with the ABAQUS modelling, along with determine whether the magnetostrictive ribbons embedded in the composite could detect failure of the composite at the surface. For each sample, the magnetisation was mapped before and after the test, and the difference in magnetisation taken.

III. Results and Discussion

A. ABAQUS Modelling

Fig. 2 shows the results for the tensile test and the 3-point

bending for a composite only panel, a panel with surface mounted ribbons and a panel with ribbons embedded in the composite. For each simulation the max force applied to achieve a displacement of 5mm was determined and a stress-strain curve, from which the overall Young's modulus can be determined. Thus, for the tensile tests, the composite panel max force applied was 8.003×10^4 N, which was lower than the surface mounted ribbons panel force of 8.077×10^4 N and the embedded ribbon panel force of 8.118×10^4 N.

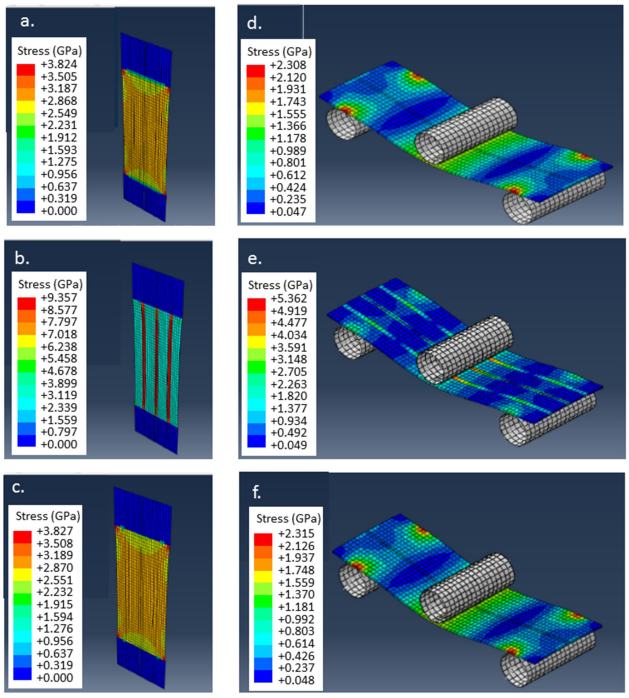

Fig. 2. ABAQUS results for the tensile test a. composite panel, b. surface mounted ribbon panel and c. embedded ribbon panel and for the 3-point bending test d. composite panel, e. surface mounted ribbon panel and f. embedded ribbons.

From the simulations shown in Fig. 2, the obtained tensile Young's modulus values were 40, 163, and 41 GPa for the no-ribbon, surface-mounted, and embedded ribbons respectively. For the 3-point bending Young's modulus these values were 40, 56.9, and 57.1 GPa respectively. These results are reasonable as they are comparable to the manufacturer's data of 52.7 GPa. The large increase in modulus value for the surface-mounted test may be due to the ribbon's properties influencing the simulation results, due to the applied forces being concentrated on the surface-mounted ribbon (the Young's modulus of the ribbon is 168 GPa, and similar to the obtained Young's modulus results). Taking the no-ribbon sample as the basis for comparison, it appears that composite properties in tension do not vary when the ribbon is embedded, as it appears that the surrounding composite fails first; meanwhile, the results of the bending simulations suggest that the material is stiffer in bending – seeing an increase of approximately 15 GPa for both surface-mounted and embedded ribbons, suggesting a strengthening effect contributed by the addition of the ribbon. The simulation results also suggest that the ribbons, when surface mounted, delaminate off the composite surface prior to failure, likely due to the vastly different mechanical properties of both materials. This was not observed to occur with the embedded ribbons.

These results are indicative of the complex structural properties of composite materials, but are not necessarily indicative of deleterious effects on the structural properties of the composite panels, as other factors may influence composite properties. The simulations also assume that the composite plys and ribbons are well-bonded to one another, which may not be true as surface bonding effects are not considered within these simulations. Furthermore, environmental effects may change the properties of fabricated components with ribbons left on during composite lifetime (*e.g.* there may be a concentration of thermal energy from the ribbons, as it possesses an increased heat capacity *vis-à-vis* the composite matrix).

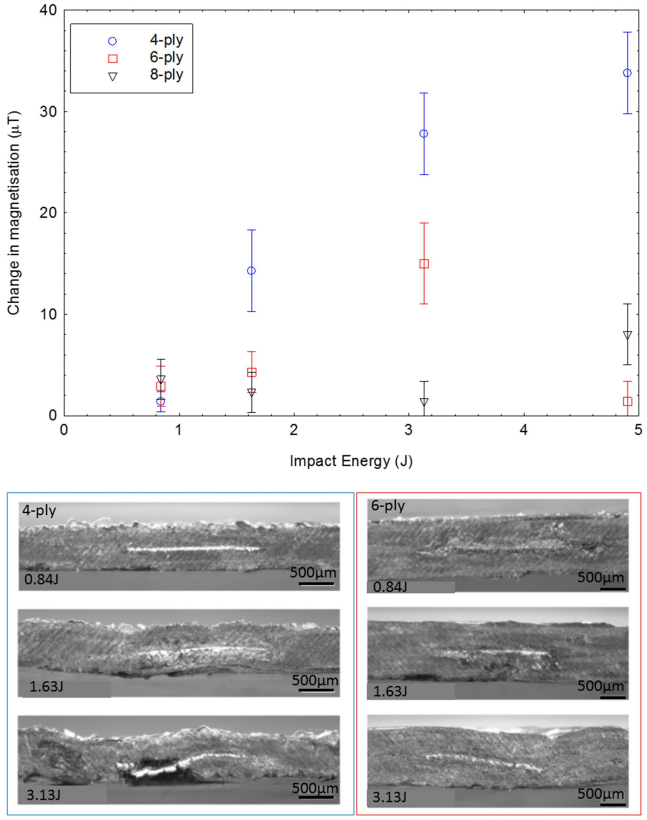

Fig. 3. Impact damage as a function of composite thickness with embedded ribbons. Images of the damage to the composite, for 4-ply (LHS) and 6-ply (RHS).

One key point is that the ribbons may delaminate from the composite surface prior to failure – alternative methods of ribbon fixation need to be considered, or alternatively, the ribbons may be embedded sub-surface, as discussed previously, to avoid surface delamination. However, further investigation here is also needed to determine the window of damage detection – and if this overlaps with the delamination window, this potential issue would need to be addressed.

B. Impact Damage

Two different impact damage detection measurements were

carried out. The first studied whether magnetostrictive ribbons embedded within the composite at different thicknesses could detect the surface impact damage and the second studied the sensitivity of the magnetostrictive ribbons attached to the surface as a function of distance of the impact damage from the ribbon. One reason to study the embedded ribbons, is from the ABAQUS modelling, the surface mounted ribbons are likely to delaminate before composite failure occurs, which is not ideal for a damage detection system.

Fig. 3 shows the impact test results for three different thicknesses of composite, with the magnetostrictive ribbon within the composite. At impact energies of 0.84 J, almost no changes in magnetisation are observed - it is expected that the impact energy is insufficient to inflict a large enough strain field to be detectable by the embedded magnetostrictive ribbons. Failure analysis of the composite panels was performed following the Tsai-Hill criterion (using the mechanical properties provided by the manufacturer), suggesting that composite failure will occur at ~375 MPa for each ply of the twill weave. It is possible to estimate the stress experienced by the composite from:

$$Stress = \left(\frac{m\,g+(m\,v^2)/(2\,s)}{A}\right) \quad (1)$$

where m is the mass of the impact tip and attached weights, g is the acceleration of gravity, v is the velocity experienced by the impact tip, s is the displacement experienced by the composite, and A is the area of the impact tip head. By estimating composite displacement from the manufacturer's provided strain to failure (1.7%), the stress experienced by the composite during impact tests may be estimated (*cf.* Eq. 1). The results for these calculations are shown in Fig. 4, suggesting that the sensitivity of the embedded sensors to damage induced from impact damage testing decreases with the number of composite plys.

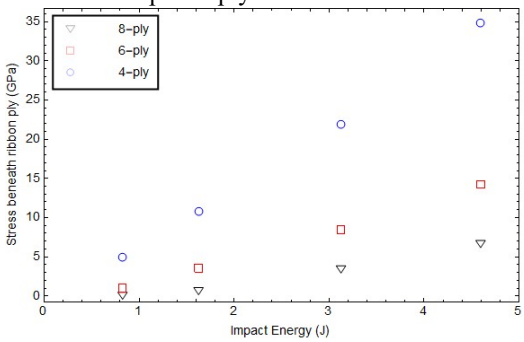

Fig. 4. Failure analysis of the internal damage that occurs after impact damage

Comparing this to the experimental results (*cf.* Fig. 3), suggests that stress experienced may be related to the change in magnetisation measured. It is observed that the change in magnetisation increases as the impact energy increases for the 4 and 6-ply, while the 8-ply shows slight changes in magnetisation (the fluctuations may be due to low sensitivity and errors), with the magnetisation increasing for the 4.9J impact. A large drop in magnetisation reading is observed for the 6-ply at 4.9J impact, which is also attributed to experimental error.

Previous results have indicated that magnetostrictive response drops rapidly as the impact position moves away from the ribbon [17], and is also shown in the results below. It is possible that an error during synthesis (uneven ribbons spacings) or drop testing (in deviations from the targeted drop position) has affected the readings. Increased thicknesses also decrease the signal-to-noise ratio as the magnetostrictive response is much lower. Nevertheless, the results are generally in good agreement with the failure analysis.

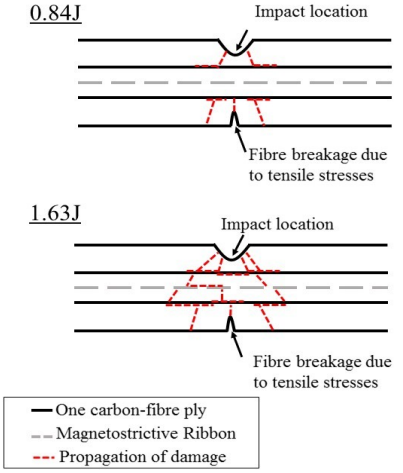

Fig. 5. Schematic of the internal damage that occurs after impact damage

In general, this means that ribbons embedded in the middle of the 6-ply and 8-ply composites are subject to more error, and may not detect impact damage on the surface. Ribbons embedded in the middle of the 4-ply appear to have no issues. Optical verification of the damages was performed on some samples (*cf.* Fig. 3); as may be expected, they indicate that the ribbon deforms within the 4-ply and 6-ply composite as a function of impact damage, and is expected to be the cause of the change in magnetisation.

Impact energies of 0.8 J cause insufficient damage to the composite to deform the embedded ribbon (Fig. 5). This means the impact damages the top composite ply, but does not penetrate further into the composite panel, as observed in the top image in Fig. 3. An energy of 1.63 J is large enough to inflict damage onto the 4-ply sample, which penetrates further than the first ply; the damage will consist of matrix cracks and delamination (Fig. 5), which propagate deep enough to strain the magnetostrictive ribbon (Fig. 3 2nd image) and thus change the ribbon's magnetisation. As the impact energy increases, so does the damage to the composite and hence the deformation of the ribbon (Fig. 3 images). From Fig. 3, the results suggest that there is a threshold impact energy for each thickness of composite (as determined from the failure analysis), which will cause a change in magnetisation within the ribbon, which may become more complex for thicker plys due to energy dissipation mechanisms. This is also observed visually in the images of the ribbon and composite after damage (*cf.* Fig. 3), as the 6-ply ribbon is only significantly deformed for 3.13 J impact energy, and not for 1.63 J energy, hence a significant change in magnetisation is observed for the 3.13 J impact (possibly due to flux leakage) in comparison to 1.63 J. These mechanisms require further investigation to optimise the sensors and are planned in follow-up studies.

Fig. 6 shows the change in magnetisation as a function of distance for different impact energies from a single ribbon. It is observed that the change in magnetisation measured on the ribbon is independent of the magnitude of the impact energy, with both impact energies causing enough damage to the surface of the composite to change the magnetisation of the ribbon. This means that impact energies above 1.6 J can be detected by a magnetostrictive ribbon. The data also shows that there is a "linear" decrease in the change in magnetisation as the distance of the impact from the ribbon increases up to 5 mm. At 5 mm, the error on the magnetisation reading is larger than the change in magnetisation reading, and therefore it is not possible to measure a change in magnetisation due to impact. From this data, it can be concluded that the distance between magnetostrictive ribbons should be no more than 10 mm; possibly less as this can impact accuracy as observed in Fig. 3 if damage is at the centre of the 10mm spacing.

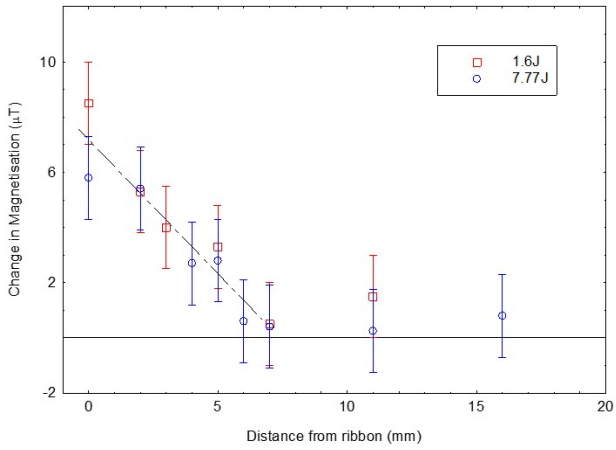

Fig 6. Change in magnetisation as a function of distance from a single surface mounted ribbon. The dashed line is a guide for the eye.

The change in magnetic properties as a function of distance is expected, as it is known that the magnetic force is proportional to the inverse of the distance, 1/x. At large distances, the dipolar moment dominates, and the magnetic force may be approximated to be inversely proportional to x^2. This behaviour may also be exploited to for the construction of an actuator that does not require manual testing (thus enabling wireless sensing). To confirm this and the distance effect, a set of parallel magnetostrictive ribbons 10 mm apart were fabricated and impact damage of 1.6 J was induced between the ribbons at distance of 1, 4, and 8 mm (labelled I_1, I_2 and I_3) away from the top-most ribbon (Ribbon 1 in Fig 7). The change in magnetisation at three different points on the panel for each impact position are presented therein. The decrease in magnetisation as a function of the distance from the impact point is again observed. For impact damage 1 mm away from ribbon 1, it is observed that the change in magnetisation is 10 μT different to the impact damage that occurred further away from this ribbon. This shows that a distance of 10 mm provides enough sensitivity to detect BVD of 1.6 J to the composite. Additional tests to determine the detectability limits for other setups are being planned.

The variance in readings may be attributed to the background field at different positions; one way of accounting for this behaviour is to account for the rate of change in the magnetisation at the different impact points – a comparison between readings taken for Ribbon 1 and Ribbon 2 may be represented by the magnetisation ratios between both, M_{R1}/M_{R2}. This result is also shown in Fig 7, and at a transition point of M_{R1}/M_{R2}, $M_{R1} > M_{R2}$. Since Ribbon 1 and Ribbon 2 are of equal length, thickness and width, and are located 10mm from one another, *ceteris paribus*, the rate of change of magnetisation should equal one another at the midpoint, *i.e.* 5mm from Ribbon 1. The calculated ratio M_{R1}/M_{R2} suggests that this centroid point determined from the magnetometer to be located at 5.6mm, which is within the experimental error and is in good agreement with the previous explanations.

Thus far, magnetostrictive actuators have been shown to be able to detect damage, but one major setback is their need for handheld measurements. Our current results demonstrate that in a two-ribbon system, the induced damage may be corelated to its position by means of measuring the magnetic response exhibited by ether ribbons. Thus, the coupling of such an actuator with built-in sensors may lead the way for the development of true wireless magnetostrictive sensors for structural health monitoring.

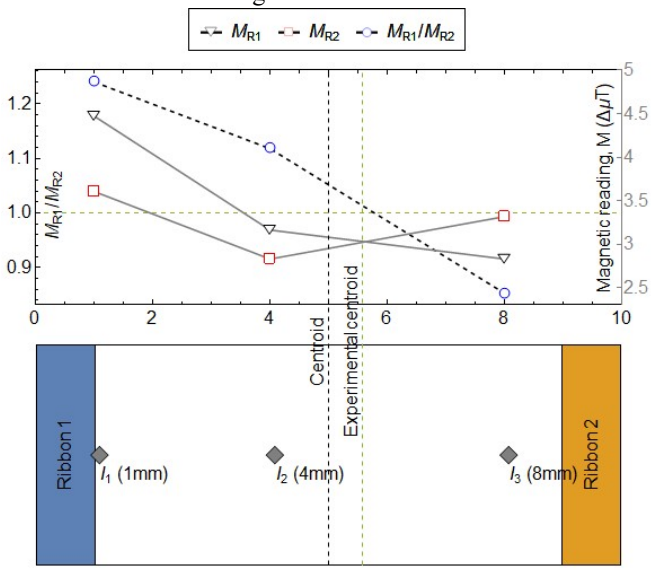

Fig 7. Magnetisation maps for surface damage, with magnetostrictive ribbons embedded within the middle of a 4-ply composite

C. 3-point Bending Measurement

Three-point bending measurements of the different thickness composite samples with ribbons embedded were carried out. The ribbons were embedded such that they would be perpendicular to the failure of the panel during the 3-point bending test. Fig. 8 shows the results for the 4-ply sample, where the top figure shows the result for no ribbons embedded and the (b) and (c) show the results for ribbons embedded. It is observed that the embedded ribbons were able to detect the failure of the composite, as a large change in magnetisation is observed along the failure line, and no change was measured near the edges of the panel. This means that the ribbons are sensitive to local composite failure, and only the part of the

ribbon magnetisation close to the damage will change. Hence the ribbons can be used to pinpoint local damage to the composite, if the magnetisation reading of the whole panel is taken. The failure of the composite only panel occurred at 531 N, with the failure for the embedded panel occurring at 507 N and 548 N, thus the embedded ribbons do not strongly change the structural behaviour of the composite panels, as predicted from the ABAQUS modelling.

For the 6-ply measurements, all samples failed, with the

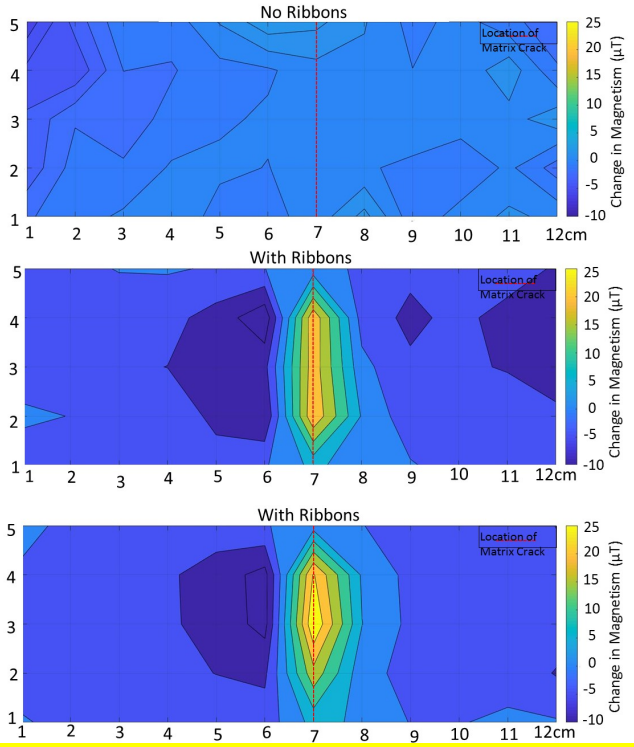

Fig 8. Magnetisation contour maps for surface damage, with magnetostrictive ribbons embedded within the middle of a 4-ply composite

composite only panel failing at 981 N, compared to 988, 905 and 1,112 N for the embedded ribbon panels. Again, this means that the addition of ribbons has not changed the structural behaviour of the composite. The contour maps after failure showed no change in magnetisation for the composite only panel, as would be expected. For the embedded ribbons panel, a change in magnetisation was measured again along the failure crack, but the magnitude of the change was 2.5 smaller than the 4-ply magnitude. This will be due to the ribbon being a further ply thickness away from the composite surface.

For the 8-ply measurements, failure occurred in the composite panel with no ribbons embedded at 1,968 N, but for the panel with ribbons embedded the max load of 2,000 N was reached with no failure occurring. For the contour maps measured after the 3-point bending for the 8-ply, no change in magnetisation was observed, as expected as no failure happened.

IV. Conclusions

ABAQUS modelling was able to predict the behaviour of the magnetostrictive ribbons attached to the surface and embedded within the composite. It showed that the ribbons take more of the stress during the measurements, and fail before the composite, i.e. delaminate from the composite surface. The modelling also predicted that the addition of ribbons within the composite do not affect the structural properties, which was confirmed experimentally using the 3-point bending test.

The best position to embed ribbons within the composite is 2-ply below the surface, as here they can detect both impact damage to the surface and composite failure. If the ribbons are embedded further into the composite, they are less sensitive to surface damage. While surface mounted ribbons detect impact damage up to 5mm away from them, but they can be damaged during the impact or delaminate.

We also demonstrate the feasibility of using a two-ribbon system to determine damage location by measuring the magnetic response across both ribbons. Such a strategy may allow actuators to be paired with *in-situ* sensors to facilitate structural health monitoring of composites *via* wireless sensing.

Acknowledgment

This work was in part funded under the Cleansky2 scheme, for the project SHERLOC JTI-CS-2009-01-GRA-01-005.

References

[1] D. D. L. Chung, “Carbon fiber composites”, Butterworth-Heinemann, pp3-4, 2012

[2] A. Quilter, Composite in Aerospace Applications White paper (online), 2001

[3] K. Diamanti and C. Soutis, “Structural Health Monitoring Techniques for Aircraft Composite Structures”, *Progress in Aerospace Science*, vol. 46, no. 8 pp.341-352, 2010

[4] R. L. Sierakowski and G. M. Newaz, “Damage Tolerance in Advanced Composites” Technomic Publishing Co. Inc. Lancaster, 1998

[5] S. Gholizadeh, “A review of non-destructive testing methods of composite materials”, *Procedia Structural Integrity*, vol. 1 pp 50- 57, 2016

[6] P. D. Pastuszak, A. Muc and M. Baski, “Methods of Infrared No-destructive Techniques: Review and Experimental Studies”, *Advanced Materials in Machine Design,* vol. 542, pp 131 – 141, 2013

[7] S. Gholizadeh, “A review of non-destructive testing methods of composite materials”, *Procedia Structural Integrity*, vol. 1, pp 050 – 057, 2016

[8] P. Duchene, S. Chaki, A. Ayadi and P. Krawczak, “A review of non-destructive techniques for mechanical damage assessment in polymer composites”, *Journal of Materials Science*, vol. 53, no 11, pp 7915-7936, 2018

[9] K. T. Lau, “Structural health monitoring for smart composites using embedded FBG sensor technology”, *Materials Science and Technology*, vol 30, no 13, pp 1642-1654, 2014

[10] M. Yeager, M Todd, W. Gregory and C. Key, “Assessment of embedded fiber Bragg gratings for structural health monitoring of composites*”, Structural Health Monitoring*, vol. 16, no 3, pp. 262-275, 2017

[11] A. Papantoniou, G. Rigas and N. D. Alexopoulos, “Assessment of the strain monitoring reliability of fiber Bragg grating sensors (FBGs) in advanced composite structures”, *Composite Structures*, vol. 93, no 9, pp 2163-2172, 2011

[12] G. F. Fernando, “Fibre optic sensor system for monitoring composite structures*” Reinforced plastics*, vol 49. No 11, pp41-49 2005

[13] W. H. Duan, Q Wang and S. T. Quek, “Application of piezoelectric materials in structural health monitoring and repair: Selected research examples” *Materials*, vol. 3, no. 12, pp 5169-5194, 2010

[14] A. S. Islam and C. K. Craig, “Damage detection in composite structures using piezoelectric materials”, *Smart Materials and Structures*, vol 3, no 3 p318, 1994
[15] A. Christopoulos, E Hristoforou, I. Koulalis and G. Tsamasphyros, “Inductive strain sensing using magnetostrictive wires embedded in carbon fibre laminates”, *Smart Materials and Structures*, vol. 23, no 8, pp. 085035, 2014
[16] A. Al-Taher, R. W. Reiss, A. D. Lafferty, S. A. Hayes, N. Lupu, I. Murgulescu and N. A. Morley, “Magnetostrictive Materials for aerospace applications”, *IOP Conf Series: Journal of Physics*, vol. 903, pp 012010, 2017
[17] Z. Leong, L. Chan, N. Walter, J. Clarke, W. Holmes, S. Hayes and N. A. Morley “Structural Health Monitoring using Magnetostrictive Sensors” accepted by IEEE Xpress 2018